Nonambipolar Magnetic-Fluctuation-Induced Particle Transport and Plasma Flow in the MST Reversed-Field Pinch

W. X. Ding,[1,2] D. L. Brower,[1,2] D. Craig,[2,3] B. H. Deng,[1] S. C. Prager,[2,4] J. S. Sarff,[2,4] and V. Svidzinski[2,4]

[1]*Department of Physics and Astronomy, University of California at Los Angeles, Los Angeles, California 90095, USA*

[2]*Center for Magnetic Self-Organization in Astrophysical and Laboratory Plasmas, University of Wisconsin-Madison, Madison, Wisconsin 53706, USA*

[3]*Department of Physics, Wheaton College, Wheaton, Illinois 60187, USA*

[4]*Physics Department, University of Wisconsin–Madison, Madison, Wisconsin 53706, USA*

(Received 10 April 2007; published 3 August 2007)

First direct measurements of nonambipolar magnetic fluctuation-induced charge transport in the interior of a high-temperature plasma are reported. Global resistive tearing modes drive the charge transport which is measured in the vicinity of the resonant surface for the dominant core resonant mode. Finite charge transport has two important consequences. First, it generates a potential well along with locally strong electric field and electric field shear at the resonant surface. Second, this electric field induces a spontaneous $E \times B$ driven zonal flow.

DOI: 10.1103/PhysRevLett.99.055004 PACS numbers: 52.25.Gj, 52.35.Py, 52.35.Vd, 52.55.Hc

Recently, there has been growing interest in plasma flow in various toroidal magnetic confinement devices. Flow in plasmas can arise from several causes. For instance, turbulence driven fluid Reynolds stresses can produce mean perpendicular flows. This is the case for zonal flows driven by electrostatic turbulence in tokamaks [1]. Alternatively, flows can also arise from radial electric fields (and resulting $E \times B$ drifts) that are produced by the differential (nonambipolar) radial transport of ions and electrons. Nonambipolar transport (charge transport) is expected to occur in the presence of stochastic magnetic fields since electrons stream rapidly along field lines. These stochastic magnetic fields can be driven by tearing instabilities [2,3], that often underlie the sawtooth oscillation, or by deliberate application of perturbing field (as in ergodic divertors) [4].

Charge flux (Γ_q) associated with magnetic stochasticity is given by the correlated product of the parallel current density fluctuations and radial magnetic field fluctuations according to

$$\Gamma_q = \Gamma_i - \Gamma_e = \frac{\langle \delta j_\parallel \delta b_r \rangle}{eB} \tag{1}$$

In this relation, Γ_i, Γ_e are magnetic fluctuation-induced ion and electron particle fluxes generally given by [5]

$$\Gamma_\alpha = \frac{\langle \delta j_{\parallel,\alpha} \delta b_r \rangle}{q_\alpha B}, \tag{2}$$

where $\langle \ldots \rangle$ denotes a flux-surface average, $\delta j_{\parallel,\alpha}$ is the species current density fluctuation parallel to the equilibrium magnetic field $\vec{B}$, and δb_r is the radial magnetic field fluctuation. The magnetic fluctuation-induced particle transport can be nonambipolar ($\Gamma_i \neq \Gamma_e$), due to the dependence on species charge (q_a).

Magnetic fluctuation-induced particle transport has been studied for many years (see [5], and references therein) but all previous measurements were made by probes and, consequently, limited to the cooler edge region of hot plasmas. In the edge, it was found that particle losses induced by magnetic field fluctuations were ambipolar [6–8]. More recent measurements suggest this may no longer hold true, as probes are inserted deeper into the plasma [9]. Theoretically, a nonambipolar flux can exist but must be balanced by an opposing nonambipolar flux to maintain plasma quasineutrality [10]. Furthermore, it has been shown that the charge flux is not pointwise zero for a localized normal mode and ambipolarity can still be realized on a spatial average [11].

In this Letter, we experimentally explore the case where magnetic field lines become stochastic during the crash phase of a sawtooth oscillation corresponding to a reconnection event in the reversed-field pinch (RFP) configuration. Magnetic fluctuation-induced charge flux related to the dominant core-resonant mode is measured directly using a nonperturbing, high-speed, laser-based Faraday rotation diagnostic. Measurements show that the radial charge flux from magnetic fluctuations alone is localized to the mode-resonant surface and is nonzero ($\sim 1\%$ of the total radial particle flux). The charge flux by itself would lead to a huge radial electric field. However, it is largely offset by the ion polarization drift across magnetic surfaces. The net result, determined from the measured magnetic fluctuation-induced flux (including the inferred polarization drift and viscous damping), is a charge separation that produces large radial electric field and radial electric field shear, leading to a $E \times B$ zonal flow at the resonant surface. This magnetic fluctuation-induced charge flux is found experimentally to depend upon nonlinear mode-mode coupling.

Measurements reported herein were carried out on the MST RFP [12,13] whose major radius $R_0 = 1.5$ m, minor radius $a = 0.52$ m, discharge current 350–400 kA, line-averaged electron density $\bar{n}_e \sim 1 \times 10^{19}$ m^{-3}, electron temperature $T_e \sim T_i \sim 300$ eV, and effective charge number $Z_{\text{eff}} = 2$–6. Equilibrium and fluctuating magnetic fields are measured by a fast ($\Delta t \sim 1$ μs) Faraday rotation diagnostic where 11 chords (separation ~8 cm) probe the plasma cross section vertically [14]. MST discharges display a sawtooth cycle in many parameters and measured quantities are ensemble (flux-surface) averaged over these reproducible sawtooth events. All fluctuation measurements refer to the dominant core-resonant resistive-tearing mode ($m/n = 1/6$ where m and n are poloidal and toroidal mode number, respectively) with laboratory frame frequency ~15–20 kHz whose resonant surface is located at $r/a = 0.35$.

Before proceeding to describe the measurements, it is useful to first express Eq. (1) in a form most suitable for experimental determination. The flux-surface averaged quantity can be rewritten as

$$\langle \delta j_\parallel \delta b_r \rangle = \langle \delta j_\phi \delta b_r \rangle \frac{B_\phi}{B} + \langle \delta j_\theta \delta b_r \rangle \frac{B_\theta}{B}, \qquad (3)$$

where ϕ, θ are the toroidal and poloidal directions, respectively. This equation can be further simplified by using Ampere's law $\nabla \times \delta B = \mu_0 \delta J$ and Gauss' law $\nabla \cdot \delta B = 0$ for a single mode, leading to

$$\langle \delta j_\parallel \delta b_r \rangle \approx \frac{1}{\mu_0} \frac{R}{nB} \left\langle \delta b_r \frac{\partial}{\partial r} \delta b_\theta \right\rangle (\vec{k} \cdot \vec{B}) \qquad (4a)$$

$$\approx \frac{1}{\mu_0} \frac{B_T}{B} \left(1 - \frac{m}{nq(r)}\right) \langle \delta j_\phi \delta b_r \rangle \qquad (4b)$$

where $\vec{k} \cdot \vec{B} = \frac{n}{R} B_\phi + \frac{m}{r} B_\theta$ ($= 0$ at the resonant surface). An additional term, $\frac{B_\phi}{B}\left(1 - \frac{B_\theta R m}{B_\phi n r}\right) \frac{\langle \delta b_r \delta b_\theta \rangle}{r}$, is not included in Eq. (4b) as it is found to be small in the vicinity of the resonant surface, $|(r - r_s)/r_s| \ll 1$, where r_s is the resonant surface location [15].

The charge flux spatial profile is determined by measuring all quantities in Eq. (4b). The radial derivative of δb_θ is directly obtained by measuring current density fluctuations ($\delta j_\phi \approx 1/\mu_0 \partial \delta b_\theta / \partial r$) using a novel polarimetry analysis technique which uses Ampere's Law to evaluate the current density between adjacent chords [14,15]. The phase information between δj_ϕ and δb_r is evaluated by ensemble averaging. In MST, rotation of the low-n magnetic modes transfers their spatial structure in the plasma frame into a temporal evolution in the laboratory frame. Since the magnetic modes are global, for convenience we correlate δj_ϕ to a specific helical magnetic mode obtained from spatial Fourier decomposition of measurements from 64 wall-mounted magnetic coils. After averaging over an ensemble of similar events, we can directly determine the phase between δj_ϕ and $\delta b_\theta(a)$ for the specified mode. Since the radial magnetic perturbation is expected to have a constant phase at all radii for tearing modes (verified by probe measurements in lower temperature plasmas), we can infer the phase between $\delta j_\phi(r)$ and $\delta b_r(r)$ knowing the phase difference between $\delta b_r(a)$ and $\delta b_\theta(a)$ is $\pi/2$ at the conducting wall. Toroidal current density fluctuations slowly increase during the linear phase of the sawtooth cycle and surge at the crash as shown in Fig. 1(a). The phase (Δ) between toroidal current density and radial magnetic field fluctuations is nearly $\pi/2$ away from the sawtooth crash, making the cosine of phase near zero as shown in Fig. 1(b). This implies the magnetic fluctuation-induced particle transport is approximately ambipolar. However, when approaching the crash, the phase deviates from $\pi/2$ and the fluctuation amplitude increases thereby generating nonvanishing magnetic fluctuation-induced charge flux. The charge flux spatial maxima over a sawtooth event is seen in Fig. 1(c), and shows a peak of $\sim 4 \times 10^{19}$ m^{-2} s^{-1} at the crash. Although the charge flux is less than 1% of the measured total radial particle flux [16], it results in a radial current ($J_r = e\Gamma_q$) which significantly impacts the plasma radial electric field.

The radial profile of $\langle \delta j_\phi \delta b_r \rangle$, which is the Lorentz force equivalent to the Maxwell stress, is shown in Fig. 2(a). Here, the radial magnetic and current density fluctuation profiles have been measured for the dominant core-resonant ($m/n = 1/6$) mode just prior to the sawtooth crash [14]. $\langle \delta j_\phi \delta b_r \rangle$ is localized near the resonant surface and has spatial extent comparable to the magnetic island

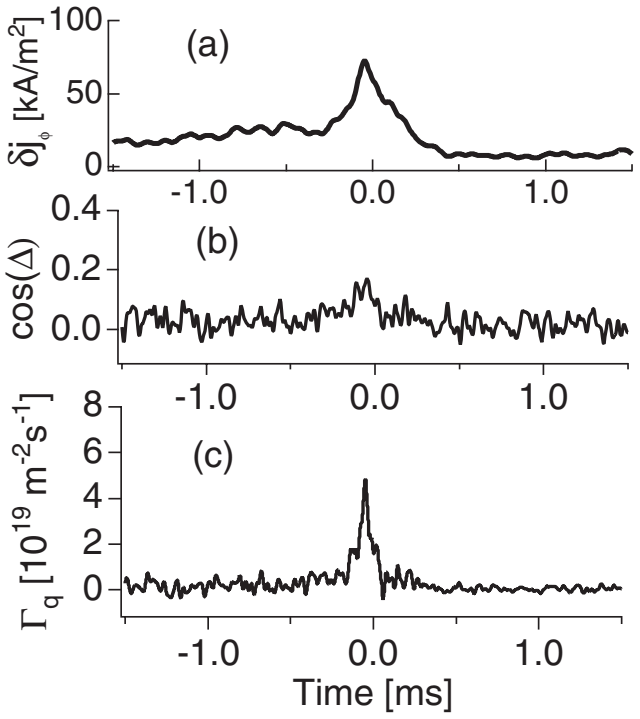

FIG. 1. (a) Current fluctuations; (b) phase between current and magnetic field fluctuation for $m/n = 1/6$ mode; (c) the charge flux. The $t = 0$ denotes sawtooth crash. Measurements are made around $r = 20$ cm, near the resonant surface.

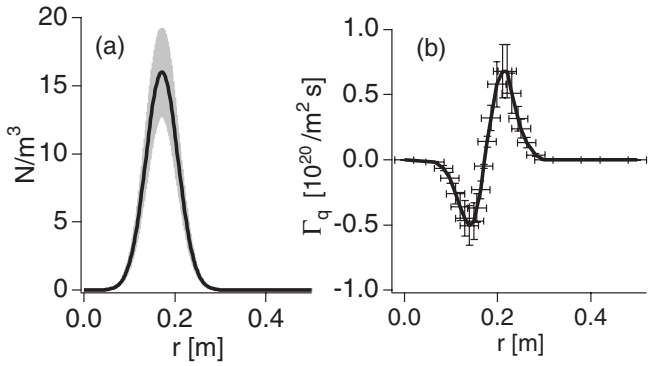

FIG. 2. (a) Spatial profile of radial derivative of Maxwell stresses. This force peaks at resonant surface with a finite width about 8 cm; (b) magnetic fluctuation-induced charge flux spatial distribution. Flux changes sign across resonant surface at $r = 0.17$ m. Data are for time $t = -0.25$ ms.

width. By combining this result with equilibrium magnetic field profile [17], we are able to obtain the spatial profile of charge flux [Eq. 4(b)] at a sawtooth crash as seen in Fig. 2(b). Charge flux is zero at the resonant surface because $\vec{k} \cdot \vec{B} = 0$. However, on either side of the resonant surface the charge flux is nonzero and changes sign due to magnetic shear (i.e., $\vec{k} \cdot \vec{B}$ changes sign across the resonant surface).

The nonvanishing charge flux indicates that the magnetic fluctuation-induced particle transport is nonambipolar, at least locally. As a consequence, plasma quasineutrality implies that large radial electric fields will quickly appear. To gain insight into the potential implications of magnetic fluctuation-induced charge flux on plasma dynamics, we use Poisson's equation and the charge conservation equation to evaluate the radial electric field (E_r) according to the relations

$$\varepsilon_0 \frac{\partial E_r}{\partial t} = \sum_j q_j \Gamma_j^r, \tag{5a}$$

$$\sum_j q_j \Gamma_j^r \approx -\varepsilon_0 \left(\frac{c}{V_A}\right)^2 \frac{\partial E_r}{\partial t} - \frac{\langle \delta j_\parallel \delta b_r \rangle}{B} - \frac{\mu}{B} \nabla^2 V_{E\times B}, \tag{5b}$$

where Γ_j^r represents the radial particle flux for j species. In Eq. (5b), we retain three contributions to the radial flux [other terms [18] in Eq. (5a), not shown here, and are estimated to be smaller than $\langle \delta j_\parallel \delta b_r \rangle / B$ for MST plasmas]. The first term is an ion polarization drift where V_A is the Aflven speed [19], the second term is the charge flux generated only by magnetic fluctuations, and the last term is the classical charge flux arising from the radial flow due to the $F \times B$ drift, where F is the viscous force within the magnetic surface perpendicular to B [11]. In the last term, μ is perpendicular viscosity coefficient and $V_{E\times B} = -E_r/B$ is a fluctuation-induced mean flow. To provide an estimate of radial electric field, numerical integration of Eq. (5b) can be performed using boundary conditions $E_r(0) = E_r(a) = 0$. The classical perpendicular viscosity $\nu^* = \mu/\rho (\sim nkT_i/\omega_{ci}^2 \tau_i)$ is determined using measured plasmas parameters, where ρ, ω_{ci}, τ_i are mass density, ion gyrofrequency, and collision time, respectively. Temporal evolution of the computed radial electrical field, driven by the measured charge flux, is shown in Fig. 3(a). The radial electric field is small and slowly increasing prior to a sawtooth crash due to a small magnetic fluctuation-induced charge flux at this time. A maximum is reached after a surge of charge flux at the sawtooth crash. Since the charge flux diminishes immediately after the crash, the radial electric field is dissipated by classical viscous damping on longer time scale ($Z_{\text{eff}} = 6$ is used in our modeling).

As shown in Fig. 3(b), the saturated radial field spatial profile [at $t = 0.1$ ms] changes sign across the resonant surface in a fashion similar to charge flux [see Fig. 2(b)]. A maximum radial electric field of ~ 2 kV/m is reached. The radial electric field points toward the resonant surface on either side, indicating that a local potential well is created. This locally strong electric field and electric field shear can be associated with spontaneous $E \times B$ driven shear flow with a finite width of ~ 5 cm [see Fig. 3(b)].

The ensemble averaged charge flux has a $m = n = 0$ nature, therefore the spontaneously driven flow is a $m = n = 0$ zonal flow. This zero-frequency flow changes sign across the tearing mode-resonant surface, thereby imparting no net momentum. An important result here is that even small magnetic fluctuation-induced charge flux can be sufficient to generate a large zonal flow structure.

The existence of nonvanishing charge flux in MST plasmas appears to require nonlinear interactions between multiple modes. Experimentally, observed changes in fluctuation amplitude [Fig. 1(a)] and phase [Fig. 1(b)] during a

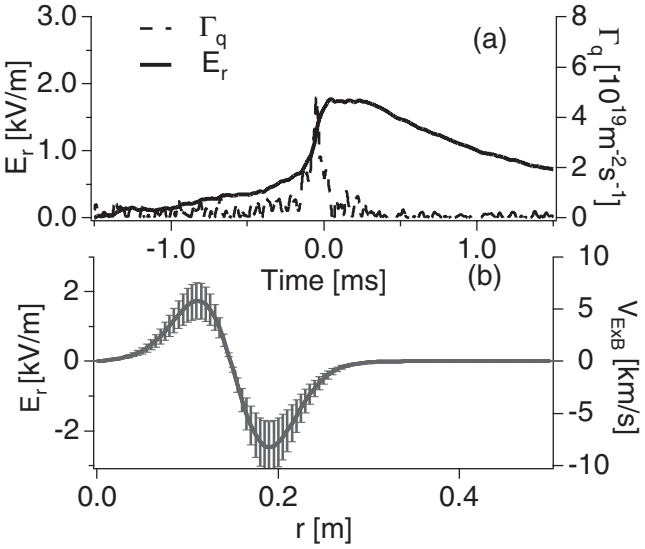

FIG. 3. (a) Radial electric field dynamics and charge flux over a sawtooth cycle. $t < 0$ corresponds to time before the sawtooth crash. (b) Radial electric field profile and $E \times B$ flow profile after sawtooth crash ($t = 0.25$ ms). The variation of B with minor radius is ignored here.

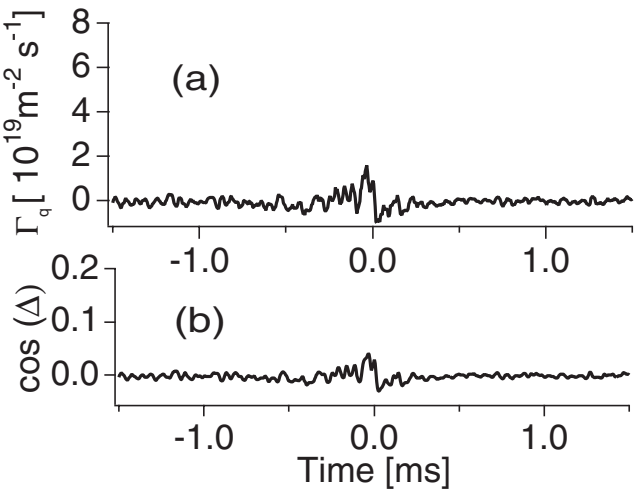

FIG. 4. (a) Magnetic fluctuation-induced charge flux dynamics over sawtooth for plasmas where $m = 0$ mode is removed; (b) phase between current fluctuations and radial magnetic field fluctuations where $m = 0$ mode is suppressed.

sawtooth crash act to drive the charge flux. In MST, resonant $m = 1$ magnetic modes dominate the core magnetic fluctuation wave number spectrum. In addition to the core-resonant modes, $m = 0$ modes (which are observed as bursts at the crash) are resonant at the reversal surface where the toroidal magnetic field goes to zero (near the plasma edge). Both the $m = 1$ and $m = 0$ tearing modes have a global nature so that nonlinear mode coupling is common. The 3-wave interaction has to satisfy the sum rule $m_1 \pm m_2 = m_3$ and $n_1 \pm n_2 = n_3$. Coupling of two adjacent $m = 1$ modes via interaction with an $m = 0$ mode has been shown to be very important in both experiments and MHD computation [20–22].

A typical strong three wave interaction observed in MST plasmas is that between the ($m = 1$, $n = 6$), (1,7), and (0,1) modes. By suppressing one of the interacting modes, we can reduce the nonlinear mode coupling. In order to identify the role played by nonlinear coupling in the charge flux during the sawtooth crash, we compare standard RFP plasmas with those where the reversal surface has been removed (i.e., nonreversed plasmas). For nonreversed plasmas, the $m = 1$ mode amplitude [$\delta b_\theta(a)$] during the sawtooth cycle remains comparable to the reversed case. However, the $m = 0$ mode amplitude is significantly reduced since its resonant surface is removed. As shown in Fig. 4(a), the charge flux for these plasmas is reduced, up to fivefold, compared to standard RFP plasmas seen earlier in Fig. 1(c). This occurs primarily because the phase difference between δj_ϕ and δb_r for the (1,6) mode is also altered, deviating only slightly from $\pi/2$, as shown in Fig. 4(b). This suggests the phase change between δj_ϕ and δb_r for the (1,6) mode is related to nonlinear mode-mode coupling.

In conclusion, tearing mode driven, nonambipolar, magnetic fluctuation-induced particle transport has been experimentally measured in the core of a high-temperature plasma. The resulting charge flux dominates in the vicinity of the resistive-tearing mode-resonant surface and reverses sign across the resonant surface. Modeling indicates the measured charge flux, including shielding from the ion polarization drift, can result in the buildup of a significant radial electric field and electric field shear. The flow pattern associated with this fluctuation-induced radial electric field has an $m = n = 0$ zonal flow structure. This flow can be dissipated on a slower time scale by classic collisions. Furthermore, we find that three wave coupling plays an important role in driving nonambipolar charge flux. Future work will focus on detection of the electric field and flow implied by the measured charge flux.

The authors acknowledge discussions with Dr. G. Fiksel and Professor C. Hegna. This work was supported by the U.S. Department of Energy and the National Science Foundation.

[1] P. H. Diamond and Y.-B. Kim, Phys. Fluids **3**, 1626 (1991); K. Itoh, S.-I. Ithoh, P. H. Diamond, T. S. Hahm, A. Fujisawa, G. R. Tynan, M. Yagi, and Y. Nagashima, Phys. Plasmas **13**, 055502 (2006).
[2] A. B. Rechester and M. N. Rosenbluth, Phys. Rev. Lett. **40**, 38 (1978).
[3] J. Wesson, *Tokamaks* (Oxford University Press, New York, 1997).
[4] K. H. Finken *et al.*, Phys. Rev. Lett. **98**, 065001 (2007).
[5] P. C. Liewer, Nucl. Fusion **25**, 543 (1985); S. C. Prager, Plasma Phys. Controlled Fusion **32**, 903 (1990).
[6] M. R. Stoneking *et al.*, Phys. Rev. Lett. **73**, 549 (1994).
[7] T. D. Rempel *et al.*, Phys. Fluids B **4**, 2136 (1992).
[8] W. Shen, R. N. Dexter, and S. C. Prager, Phys. Rev. Lett. **68**, 1319 (1992).
[9] Neal A. Crocker, Ph.D. dissertation, University of Wisconsin, Madison, 2001.
[10] T. E. Stringer, Nucl. Fusion **32**, 1421 (1992).
[11] R. E. Waltz, Phys. Fluids **25**, 1269 (1982).
[12] R. N. Dexter *et al.*, Fusion Technol. **19**, 131 (1991).
[13] H. A. B. Bodin, Nucl. Fusion **30**, 1717 (1990).
[14] W. X. Ding *et al.*, Rev. Sci. Instrum. **75**, 3387 (2004).
[15] W. X. Ding *et al.*, Phys. Rev. Lett. **90**, 035002 (2003).
[16] N. E. Lanier *et al.*, Phys. Plasmas **8**, 3402 (2001).
[17] S. D. Terry *et al.*, Phys. Plasmas **11**, 1079 (2004).
[18] K. Itoh and S. Itoh, Plasma Phys. Controlled Fusion **38**, 1 (1996).
[19] S. Inoue, T. Tange, K. Itoh, and T. Tuda, Nucl. Fusion **19**, 1252 (1979).
[20] A. K. Hansen *et al.*, Phys. Rev. Lett. **85**, 3408 (2000); S. Assadi, S. C. Prager, and K. L. Sidikman, Phys. Rev. Lett. **69**, 281 (1992).
[21] R. G. Watt and R. A. Nebel, Phys. Fluids **26**, 1168 (1983).
[22] T. Bolzonella and D. Terranova, Plasma Phys. Controlled Fusion **44**, 2569 (2002).